Available online at www.sciencedirect.com

ScienceDirect

Scripta Materialia 99 (2015) 57–60

Scripta MATERIALIA

www.elsevier.com/locate/scriptamat

Deformation mechanisms of a nickel-based single-crystal superalloy during low-cycle fatigue at different temperatures

X.G. Wang,[a] J.L. Liu,[a] T. Jin,[a,*] X.F. Sun,[a] Y.Z. Zhou,[a] Z.Q. Hu,[a] J.H. Do,[b] B.G. Choi,[b] I.S. Kim[b] and C.Y. Jo[b]

[a]*Superalloys Division, Institute of Metal Research, Chinese Academy of Sciences, 72 Wenhua Road, Shenyang 110016, China*
[b]*High Temperature Materials Research Group, Korea Institute of Materials Science, 797 Changwondaero, Changwon, Gyeongnam 641-831, Republic of Korea*

Received 4 November 2014; revised 24 November 2014; accepted 25 November 2014
Available online 9 December 2014

Deformation mechanisms of an Ni-based superalloy during low-cycle fatigue at various temperatures were studied. A new configuration of cross-slip dislocation was observed in the γ matrix during the deformation at 760 and 900 °C, which is an important component of the slip band at 900 °C. Slip bands with different morphologies were observed at room temperature and 900 °C, corresponding to the obvious work-hardening. It was observed that stacking faults spread throughout the γ/γ′ interface.

Keywords: Low-cycle fatigue; Slip band; Dislocation configuration; Ni-based superalloy

It is well known that the microstructure of Ni-based single-crystal (SX) superalloys consists of two phases: ordered intermetallic γ′ precipitates with an $L1_2$ structure coherently embedded in a disordered face-centered cubic (fcc) γ matrix [1–4]. Because of this unique microstructure, superalloys exhibit unique temperature-dependent strength properties under simple monotonic loading [2–6]. On the other hand, because these superalloy components are subjected to cyclic thermal stresses resulting from startup and shutdown, mechanical fatigue has been an area of ever-growing interest for the past several decades [7–10]. Compared to low-cyclic fatigue (LCF), thermomechanical fatigue (TMF) can approach the real conditions of these superalloys during service and evaluate fatigue damage effectively. Nevertheless, because the TMF behavior is complex and it is difficult to control the variables precisely, isothermal LCF has been frequently used to predict the damage behavior and fatigue life.

The development of a life prediction scheme requires a proper understanding of LCF damage mechanisms. Therefore, it is important to understand the LCF deformation mechanisms at various temperatures. Planar slip is considered as a dominant deformation mode at room temperature (RT), and the slipping dislocations are restricted in the parallel slip bands (SBs) [11,12]. Li et al. [7] found that the dislocation configuration became homogeneous with increasing temperature, and the SBs gradually disappeared. However, Petrenec et al. [13] found that the SBs are always present across the entire medium-temperature range (600–800 °C). In other words, the LCF deformation mechanisms become more complex in the medium-temperature range. Over 800 °C, SBs usually cannot be observed, and the deformation microstructures become more homogeneous. The change in deformation mechanisms must be related to the chemical composition, size and volume fraction of the γ′ precipitates and deformation conditions. On the other hand, it is well known that the stacking fault energy (SFE) significantly affects deformation mechanisms [14]. Although the SFE of pure Ni is as high as $200\ mJ \cdot m^{-2}$ [15], the SFE values of the γ and γ′ phases significantly decreased with the addition of various elements (e.g. Co, Re and Ru) [15,16]. Thus, it is useful to study the deformation mechanisms of SX superalloys with a low SFE. In turn, the study may promote the development of alloy design. However, little work has been conducted on this aspect.

In this work, an experimental SX superalloy with a low SFE was used to study the LCF deformation mechanisms at various temperatures. The nominal chemical composition was as follows: 12Co, 6Al, 19.4(Cr + Mo + W + Ta), 5.4Re, 3Ru and balance Ni (in wt.%). The preparation and heat treatment of this alloy have been described elsewhere [17]. The cylindrical specimens of the alloy along the [001] direction for the LCF tests have a gauge length of 15 mm and a diameter of 6 mm. Before the LCF tests,

* Corresponding author. Tel.: +86 24 2397 1757; fax: +86 24 2397 1758; e-mail: tjin@imr.ac.cn

http://dx.doi.org/10.1016/j.scriptamat.2014.11.026
1359-6462/

mechanical and electrochemical polishing of all the specimens were conducted to prevent premature crack initiation at the surface-machined scratches. The LCF tests were conducted under controlled total strain ($\Delta\varepsilon t = 1.6\%$) in air at RT and 760, 900 and 980 °C, using a MTS810 servo-hydraulic testing machine. A triangular waveform with a constant strain rate of 5×10^{-3} s^{-1} and a strain ratio of $R = -1$ was used. Transmission electron microscopy specimens were prepared from undeformed and deformed samples by conventional grinding and polishing in a solution of 20 vol.% perchloric acid and 80 vol.% methanol at a temperature of −25 °C and a voltage of 20 V. The microstructures were examined using a JEM-2100F scanning transmission electron microscope operating at 200 kV.

Figure 1 shows the micrograph of the γ/γ′ structure of the experimental alloy after heat treatment. The volume fraction of the γ′ precipitates is approximately 70%, and average length of the cube edge is approximately 0.3 μm. Stacking faults (SFs) were occasionally observed to be present in the γ matrix, indicating that this alloy has a very low SFE. The driving force for the SF formation may be related to the misfit energy.

Figure 2 shows the microstructural configurations of the experimental alloy after LCF deformation at RT (Fig. 2a) and 760 °C (Fig. 2b and c). Some SFs are present in both the γ and γ′ phases (Fig. 2a). The formation of these SFs in the γ′ phase during LCF deformation has been widely reported [7–9]. However, the SFs present in the γ matrix have been rarely reported previously, particularly at low temperature (e.g. RT). The occurrence of these SFs in the two phases indicates that the SFE of this alloy is very low. Thus, it is difficult for a dislocation to cross-slip in the {111} slip planes and planar slip is considered to be the dominant deformation mechanism in the low-temperature range [11,18]. The observation of an SB (Fig. 2a) is good evidence for the above conclusion. This SB mainly consists of a high density of tangled dislocations planar slipping in the matrix and continuously cutting through the γ′ phase [7,13]. A number of ladder-like structural SBs parallel to the {111} slip planes have been reported at RT [7,13]. However, in this alloy, an SB was only occasionally observed under the present LCF conditions. In other words, the deformation inhomogeneity of this alloy is not very severe compared to other superalloys [11,15,18]. Moreover, the configuration of these dislocations does not differ significantly with that after tensile deformation and is considered to be $a/3\langle 112\rangle$ type (under some operation vectors, SF and the dislocation can be observed simultaneously) [17]. At 760 °C, no SF in the γ′ phase and SB in the sample were observed (Fig. 2b and c). Thus, the dislocations in the γ′ phase are considered to be $a/2\langle 101\rangle$ type (the tilting results support this conclusion). In other words, the antiphase domain boundary (APB) energy is more favorable than the SFE in the γ′ phase under the present LCF deformation conditions. However, the SFs still present in the γ matrix and the different extending directions indicate that multiple slips were activated.

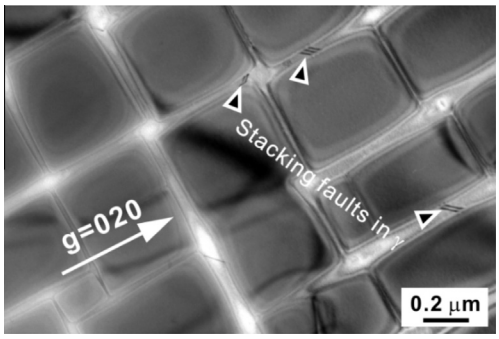

Figure 1. Microstructure of the experimental alloy after heat treatment. The image was taken close to the [001] zone axis.

Here, a very interesting and new dislocation configuration was observed, as shown in Figure 2c. To the best of our knowledge, this type of dislocation configuration has rarely been reported. In the configuration, several obvious characteristics can be observed in the dislocations: (i) the traces of these dislocations show a zigzag contrast and usually have 90° reorientation, indicating that cross-slip has occurred; (ii) the distance between the two parallel dislocations is small and approximately 35 nm in width after being projected on the (001) plane, as marked by paired arrows and a capital letter "W"; (iii) the dislocations seen can pass through the γ/γ′ interface easily at the position "N"; and (iv) complex reactions may have occurred in the vicinity of "A". By carefully analyzing the above-mentioned dislocation characteristics, it is concluded that this type of dislocation configuration may have resulted from the cross-slip of the screw dislocation segment on the {111} slip planes in the horizontal γ matrix, and leaving the paired 60° dislocations at the γ/γ′ interface. This formation process is schematically illustrated in Figure 2d. The actual distance between the two parallel 60° dislocations ("R") and the width of the γ matrix ("H") can be calculated using the geometrical relationship with "W", as shown at the bottom right of Figure 2d. The calculation results show that "R" and "H" are approximately 60 and 50 nm, respectively. Undoubtedly, the width of the γ matrix calculated in this study is consistent with the statistical result. Thus, it can be considered as good evidence for the above conclusion. Notably, the distance between the two parallel 60° dislocations during LCF at this temperature range is much smaller than that during the high-temperature creep [2,19]. The main reason is that the proportion of dislocation climbing caused by the thermal activation during LCF is very small compared to that during the creep at elevated temperatures. Another feature of this type of dislocation should not be neglected: the length between two 90° cross-slip positions, as marked by "L", is shorter than that after the creep. It can be explained from the change in the external stress between tensile and compression, moving the leading screw dislocation forward or backward. This case is similar to the formation process of twins during TMF [10]. The forward and backward movements of the twinning dislocations result in the occurrence of twinning and detwinning processes. In fact, although the dislocation configuration is slightly different from the typical wavy slip [7], it still belongs to the category of wavy slip. In other words, the deformation mechanism gradually changed from planar slip to wavy slip as the temperature increases from RT to 760 °C. Finally, it should be noted that this type of dislocation configuration is only present in some areas, with other areas remaining free of this type of dislocation, as shown in Figure 2b.

The microstructure of the experimental alloy after the LCF test at 900 °C is shown in Figure 3a and b. SFs are still present in the γ matrix, as shown in Figure 3a. Interestingly, the SFs with different extending directions are present